Journal of Volcanology and Geothermal Research 188 (2009) 162–172

Contents lists available at ScienceDirect

Journal of Volcanology and Geothermal Research

journal homepage: www.elsevier.com/locate/jvolgeores

Boron isotopic variations in NW USA rhyolites: Yellowstone, Snake River Plain, Eastern Oregon

Ivan P. Savov [a,d,*], William P. Leeman [b,*], Cin-Ty A. Lee [c,1], Steven B. Shirey [d,2]

[a] School of Earth and Environment, University of Leeds, Leeds LS2 9JT, United Kingdom
[b] Earth Science Division, National Science Foundation, Arlington, VA 22230, USA
[c] Department of Earth Science, Rice University, Houston, TX 77005, USA
[d] Department of Terrestrial Magnetism, Carnegie Institution of Washington, Washington, DC 20015, USA

ARTICLE INFO

Article history:
Received 20 May 2008
Accepted 6 March 2009
Available online 26 March 2009

Keywords:
Boron isotope ratios
rhyolite
Yellowstone
Snake River Plain
High Lava Plains
hotspot volcanism

ABSTRACT

The geochemistry of NW USA rhyolites correlates strongly with geography and the nature of the underlying basement terranes. Rhyolites from the Snake River Plain-Yellowstone (SRPY) province have higher $^{87}Sr/^{86}Sr$, $^{207}Pb/^{206}Pb$, and lower $^{143}Nd/^{144}Nd$ than those from the Oregon High Lava Plains (HLP) province, reflecting a dominant influence of Precambrian cratonic crust east of the western Idaho suture zone versus accreted oceanic terranes of Phanerozoic age to the west. Rhyolites from the cratonic domain show significant enrichments of Th, U, and LREE/HREE, whereas B concentration and especially B/Nb and B/Rb are systematically higher west of the tectonic boundary. This decoupling of B from the other incompatible elements is best explained in terms of distinctive magmatic sources east and west of the suture zone.

B isotopic composition [$\delta^{11}B$] was measured for natural and synthetic glasses via multiple multiplier laser ablation-ICP-MS. $\delta^{11}B$ values are systematically lighter in SRPY rhyolites (−5.6 to −8.9 ‰) compared to those from the HLP (−0.8 to −3.1 ‰). These data are consistent with strongly fluid-depleted and/or metamorphosed sources for SRPY rhyolites, whereas HLP sources resemble those of typical oceanic basalts, and could reflect melting of juvenile basalt-derived protoliths in the crust. B isotope ratios of low-$\delta^{18}O$ rhyolites are indistinct from those with normal $\delta^{8}O$, suggesting that $\delta^{11}B$ values are not strongly affected by hydrothermal processes that alter source materials with meteoric water. Considering all data, it is likely that B compositions of the rhyolites are inherited from their sources in the crust. Although low $\delta^{11}B$ (<0 ‰) is also observed in many mantle-derived basalts (i.e., OIB, MORB), in SRPY rhyolites it is associated with enrichments of elements (e.g., U, Th, Rb, LREE) typically concentrated in continental crust, and thus old high-grade metamorphic continental crust is inferred to be ^{11}B-depelted. If rhyolite protoliths were originally metasediments, it is likely that bulk B and $\delta^{11}B$ were selectively removed by metamorphic dehydration reactions and transported to the surface via ^{11}B-enriched fluids.

1. Introduction

Understanding the origin of Neogene magmatism in the northwestern USA is complicated by the juxtaposition of diverse tectonic systems (cf. Oldow et al., 1989). The region has been affected by long-term convergent margin tectonism including accretion of oceanic terranes to cratonic North America outboard of the western Idaho suture zone (WISZ; Fig. 1) and formation of Cretaceous to modern arc magmatic belts culminating with the Cascadia subduction zone and volcanic arc. Following the advent of Columbia River flood basalt volcanism (ca. 16 Ma; Camp and Ross, 2004), migration of the North American plate over the Yellowstone "hotspot" produced a diachronous trail of large silicic volcanic centers that initiated in northernmost Nevada and southeasternmost Oregon. This magmatism subsequently migrated some 600 km across the Snake River Plain in southern Idaho to its present-day focus in the Yellowstone area (Pierce and Morgan, 1992; Bonnichsen et al., 2008). Over the same time interval, complementary (albeit volumetrically subordinate) silicic volcanism swept in a northwesterly direction across the High Lava Plains of southeastern Oregon toward Newberry Volcano and the Cascades volcanic arc (MacLeod et al., 1976; Jordan et al., 2004). Since Miocene time this region has also been affected by northward encroachment of the Basin and Range extensional province, and magmatism may be partly a consequence of this influence.

In the Snake River Plain-Yellowstone (SRPY) province, early activity at each eruptive center was dominantly rhyolitic for some

* Corresponding authors. Savov is to be contacted at School of Earth and Environment, University of Leeds, Leeds LS2 9JT, United Kingdom. Tel.: +44 133 343 5199; fax: +44 133 343 5259. Leeman, Earth Science Division, National Science Foundation, Arlington, VA 22230, U.S.A. Tel.: +1 703 292 8554; fax: +1 703 292 9025.
E-mail addresses: i.savov@see.leeds.ac.uk (I.P. Savov), wleeman@nsf.gov (W.P. Leeman), ctlee@rice.edu (C.-T.A. Lee), shirey@dtm.ciw.edu (S.B. Shirey).
[1] Tel.: +1 713 348 5084; fax: +1 713 348 5214.
[2] Tel.: +1 202 478 8473; fax: +1 202 478 8821.

0377-0273/$ – see front matter © 2009 Elsevier B.V. All rights reserved.
doi:10.1016/j.jvolgeores.2009.03.008

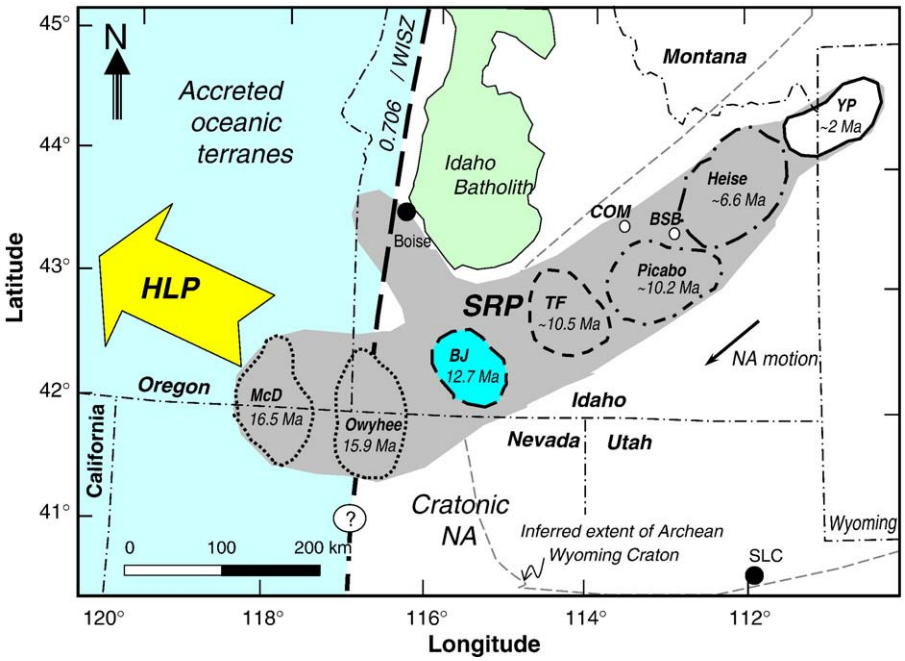

Fig. 1. Map showing locations of the Snake River Plain (SRP), Yellowstone Plateau (YP), and the High Lava Plains (HLP) provinces. Eruptive centers (or caldera clusters; cf. Pierce and Morgan, 1992) associated with migration of North America over the Yellowstone hot spot are outlined as follows (with age of earliest rhyolites in M yrs): McDermitt (McD, 16.5), Owyhee (15.9), Bruneau-Jarbidge (BJ, 12.7), Twin Falls (TF, 10.5), Picabo (10.2), Heise (6.6), and Yellowstone (YP, 2.0); rhyolites from these centers define the "main trend" of silicic volcanism in this province. Quaternary silicic rocks from Craters of the Moon (COM) volcanic field and Big Southern Butte (BSB) dome complex are also considered in this study. Rhyolites in southeastern Oregon erupted from smaller distributed vents that generally become younger to the northwest as symbolized by broad white arrow. The western Idaho suture zone (WISZ) and the $^{87}Sr/^{86}Sr = 0.706$ isopleth sharply demark the boundary between cratonic North America to the east and Paleozoic and younger accreted oceanic terranes to the west; the boundary becomes diffuse in northern Nevada owing to superimposed Neogene Basin and Range extension. The main body of the Cretaceous–Eocene Idaho batholith is shown as well as the boundary of inferred Archean basement (Wyoming craton) underlying much of southern Idaho. Small vector shows absolute motion of the North American (NA) plate. Locations of Boise and Salt Lake City (SLC) are shown for reference.

2–4 Ma. Following this "main phase" of silicic volcanism, magmatism shifted to a dominantly basaltic mode that continued intermittently across much of the province — in places, up to Holocene time. In contrast, magmatism west of the WISZ was essentially bimodal from the onset (cf. Draper, 1991; Streck and Grunder, 2007). These distinct surface manifestations undoubtedly reflect differences in the underlying lithospheric architecture, average compositions of the respective crustal domains, and magnitudes of mantle-derived magma fluxes. The main focus of this paper is on origin(s) of the silicic magmas. Silicic volcanism commonly is inferred to be driven by injection of hot basaltic magma into sialic crust (e.g., Tamura and Tatsumi, 2002; Annen and Sparks, 2002; Annen et al., 2006), or by differentiation from parental mafic magmas (McCurry et al., 2008). The relative contributions of these processes can be constrained by radiogenic isotopes and trace element modeling, yet contributions from fluids or hydrothermally altered crust remain poorly understood. This information is critical to understanding the overall energetics and scale of the underlying magmatic processes. We approach the problem of fluid contributions from the perspective of boron geochemistry based on results of a reconnaissance B isotopic investigation. Principal goals of this paper are to document spatial variations in boron systematics for NW USA rhyolites and to evaluate (a) the effects of meteoric or hydrothermal fluids on their B isotopic composition and (b) the utility of B isotope systematics as a tool for understanding rhyolite petrogenesis.

2. Boron and B isotopes

The rationale for this study is based on the facts that B is an extremely fluid-mobile element (Palmer and Swihart, 1996; Ryan et al., 1996; Ishikawa and Tera, 1997; Savov et al., 2004, 2007a), and its isotopic composition is useful in characterizing fluid sources or, more specifically, the reservoir rocks with which the fluids have interacted (cf. Palmer and Sturchio, 1990; Pennisi et al., 2000). Available partitioning studies suggest that B is most strongly hosted in phyllosilicate minerals but generally behaves as a strongly incompatible element, favoring silicate melts over all common mantle and crustal phases with the exception of tourmaline (Palmer and Swihart, 1996; Marschall et al., 2007). It is even more strongly partitioned into aqueous fluids relative to silicate melts (Savov et al., 2004, 2007a).

Boron isotopic fractionation is less well quantified, but appears to be controlled primarily by speciation that is strongly pH-dependent (cf. Spivack et al., 1987; Tonarini et al., 2001; Hervig et al., 2002). At neutral to acidic pH, boron dominantly occurs in trigonal coordination ($B\,[OH]_3$) in common solid, melt and fluid phases. Under these conditions, isotopic fractionation is small to negligible (Palmer and Swihart, 1996; Klochko et al., 2006). With increasingly basic pH, a significant fraction of the available B becomes tetrahedrally coordinated ($B\,[OH]_4^-$) in mineral phases or on mineral surfaces, whereas in coexisting melts or fluids it remains dominantly trigonally coordinated. Under these conditions (e.g., Boschi et al., 2008), selective uptake of ^{11}B in trigonal coordination can result in significant isotopic fractionation with fluids having higher $^{11}B/^{10}B$ (or $\delta^{11}B$ values; defined as $1000*[^{11}B/^{10}B_{sample}/^{11}B^{10}B_{standard} - 1]$; where $B_{standard}$ is NIST SRM 951 [boric acid]). In high temperature (magmatic) systems, the effects of fractional crystallization or melting on magmatic $\delta^{11}B$ are expected to be small when pH is neutral to acidic (as is commonly the case); however, isotopic compositions of crustal protolith rocks may retain distinctive compositions inherited from their depositional or metamorphic histories (Marschall et al., 2007).

Over geologic time such processes have led to distinctive isotopic signatures: (1) strong concentration of ^{11}B in seawater (current $\delta^{11}B_{seawater} = +40\,‰$; Spivack et al., 1987; Klochko et al., 2006), (2) B- and ^{11}B-depletion in the upper mantle ($B < 0.5$ ppm; $\delta^{11}B \sim -10$ to

−5‰) (Chaussidon and Jambon, 1994; Chaussidon and Marty, 1995; Ryan et al., 1996), and (3) elevated concentration but very light B in continental crust and marine sediments (δ^{11}B ~ −20 to −5‰) (Ishikawa and Nakamura, 1993; You et al., 1995). Locally, subduction processes can recycle marine boron back into the mantle, leading to re-enrichment of ^{11}B in sources for arc volcanic rocks (Ishikawa and Nakamura, 1993; Ishikawa and Tera, 1997; Tonarini et al., 2001; Savov et al., 2007a). This effect depends on the efficiency of dehydration processes that liberate fluids and boron from rock assemblages in the subducted slab, and hence, on the thermal structure of subduction zones (Leeman, 1999; Leeman et al., 2004). Thus, arc lavas associated with warm subduction zones tend to have low, mantle-like δ^{11}B [e.g., <0‰ for Cascades arc (Leeman et al., 2004) and 1–4‰ for W. Mexican Volcanic Belt (Savov et al., 2007b)], whereas those associated with cool subduction zones have higher δ^{11}B values (e.g., up to +16 ‰ for S. Sandwich arc; Tonarini et al., 2004).

For western USA rhyolites, only limited B isotopic data have been reported. Most significant to this study is a detailed investigation of rhyolites from the Long Valley-Inyo Craters volcanic field, in which data were obtained by SIMS analyses of melt inclusions in quartz phenocrysts (Schmitt and Simon, 2004). An important aspect of that study is that little difference in δ^{11}B was observed between water-rich melt inclusions and degassed matrix glasses. This result suggests that there is insignificant B isotopic fractionation associated with volatile losses from magmas under continental crustal conditions, even though their absolute B content may decrease. Thus, the large range in δ^{11}B observed (0 to +8‰) cannot be attributed solely to degassing processes (cf. Hervig et al., 2002), and likely reflects open-system mixing between low-δ^{11}B (e.g., crust- or mantle-derived) and high-δ^{11}B end-members (e.g., subduction-derived fluids or melts). One scenario to explain the observed range in δ^{11}B that is consistent with other isotopic data involves cannibalization of older, ^{11}B-depleted hydrothermally altered intrusive rocks by newly emplaced fresh rhyolitic magmas. This is commonly invoked to explain low δ^{18}O silicic magmas elsewhere (cf. Bacon et al., 1989).

Leeman et al. (2004) report B isotopic data for recent dacites from Mount St. Helens, in the southern Washington Cascades. These lavas have δ^{11}B (ca. −2 ‰) essentially similar to proximal basaltic magmas in the frontal arc region. These δ^{11}B values are relatively low for arc magmas, and they decrease to even lower values (−8 to −10 ‰) in the backarc region. Because the Cascade and W. Mexico volcanic arcs are associated with the warmest modern subduction zones, it appears that the slabs there have undergone significant B-depletion via shallow devolatilization in the forearc regions (Leeman et al., 2004; Savov et al., 2007a). Compared to cooler subduction regimes, low δ^{11}B in these arc magma sources could result from a relatively weak input of slab-derived B, such that compositions of Cascades and W. Mexican Volcanic Belt lavas reflect an intrinsically OIB- or MORB-like B composition of the mantle. In contrast, distinctively higher δ^{11}B in the Long Valley-Inyo rhyolites suggests that their source regions were modified by a relatively ^{11}B-rich fluid or melt inputs derived from the subducted older (more altered) and cooler Farallon slab.

In addition, judging from the Cascades arc data, it is unlikely that slab-derived fluids from this system significantly influenced compositions of mantle rocks beneath the far back arc, including the HLP-SRPY areas of our study (Fig. 1). Limited B isotopic data for Yellowstone rhyolites (Palmer and Sturchio, 1990) support this notion; one fresh and one altered sample from the Middle Geyser Basin have relatively low δ^{11}B values (−5.5 and −9.7‰, respectively). However, rhyolite lavas from this locality exhibit anomalously low δ^{18}O that has been attributed to incorporation of either hydrothermally altered caldera roof rocks (preferred interpretation) or hydrothermal fluids (less likely) into a residual silicic magma body following the caldera-forming eruption of the Lava Creek Tuff (Hildreth et al., 1984; Bindeman and Valley, 2000, 2001a,b). Although the available B isotope data might be interpreted to suggest that post-eruptive hydrothermal alteration could lower δ^{11}B, this would be surprising, considering that little isotopic fractionation is predicted for low- to moderate- pH geothermal environments like that at Yellowstone (Lowenstern and Hurwitz, 2008). Thus, the extent to which the data of Palmer and Sturchio's data represent compositions of Yellowstone rhyolite magma is unclear.

3. Samples

The present study aims to determine both the magmatic B composition of NW USA rhyolites, and the extent to which they may be influenced by hydrothermal or other secondary processes. Where possible we analyzed the freshest available obsidian glasses to minimize effects of hydration or post-eruptive alteration. The samples studied are geographically distributed from the Yellowstone Plateau (NW Wyoming) to Newberry volcano (central Oregon), and span the juncture of cratonic North America (beneath southern Idaho and Wyoming) with allochthonous accreted terranes to the west (beneath eastern Oregon). Samples from Oregon represent three Mio-Pliocene (7.5–3.6 Ma) dome-flow complexes and the Holocene (1250 ka) Big Obsidian flow from Newberry Crater. At Yellowstone we focus on samples that post-date the voluminous (~1000 km^3) Lava Creek Tuff (erupted at 0.64 Ma); these include young extra- and intra-caldera lavas (denoted as Y-EC or Y-IC, respectively) for which extremely fresh glassy samples are available. These groups are distinctive in terms of radiogenic isotope and trace element compositions, with Y-EC lavas having the strongest 'crustal signature' (see discussion below). In addition, one of the Y-IC rhyolites (Canyon flow) has among the lowest δ^{18}O values (0.2 ‰) observed at Yellowstone (Hildreth et al., 1984; Bindeman and Valley, 2000, 2001a). The samples we selected for analysis are considered representative of all important compositional variants recognized to date.

For comparison we also analyzed representative glassy rhyolites from the older (12.7–8.0 Ma) Bruneau-Jarbidge (BJ) eruptive center in the west-central SRP southwest of the Yellowstone Caldera (Fig. 1). BJ rhyolites have systematically low δ^{18}O that can only be explained in terms of strong ^{18}O-depletion of a voluminous source region (Taylor and Sheppard, 1986; Boroughs et al., 2005). Foundering of hydrothermal roof rocks, as proposed for Yellowstone (Bindeman and Valley, 2000, 2001a,b), is an unlikely explanation for the observed pervasive ^{18}O-depletions because even the earliest BJ ignimbrite shows this feature. Moreover, BJ bulk rocks exhibit unique temporal variations in composition (FeO* and TiO_2 increase, SiO_2 and incompatible elements decrease with time); these trends may reflect either progressive fractional melting of a crustal source or increasing contributions of mafic melt input over time (Leeman et al., 2008). Several ignimbrites spanning much of this compositional-age range were analyzed to evaluate possible variability in B composition. The Yellowstone and BJ rhyolites are representative of the diachronous early, or "main phase", SRPY silicic volcanism.

We also analyzed several SRP silicic samples for which derivation from associated basaltic magmas has been proposed. These include one highly evolved rhyolite obsidian from the 0.3 Ma Big Southern Butte dome complex in the eastern SRP and one ~2 ka latitic obsidian from the Devils Orchard flow at Craters of the Moon volcanic field. Leeman et al. (1976) suggested that the latite magma was produced by extreme fractional crystallization of evolved ferrobasaltic magma coupled with minor crustal contamination. McCurry et al. (2008) propose that the evolved BSB rhyolite also could be a product of extreme fractional crystallization of typical SRP basaltic magmas based partly on Sr–Nd–Pb isotopic similarities between the two; it is also possible that this rhyolite formed by partial remelting (at crustal depths) of either basaltic intrusive equivalents or advanced differentiation products of basaltic magma. To facilitate further evaluation of basaltic contributions to SRP silicic magmatism we also present

compositional data for two primitive basaltic lavas from the eastern SRP (Leeman et al., 2009).

Finally, we report new data for a single rhyolite obsidian from Mono Craters (CA; cf. Castro and Mercer, 2004). This sample was included mainly for comparison with the previously published SIMS B isotopic work on rhyolites from the Long Valley area (Schmitt and Simon, 2004). Table 1 presents selected information for all samples investigated in this study.

4. Analytical methods

New major and selected trace element data were obtained by a combination of X-ray fluorescence (XRF), instrumental neutron activation analysis (INAA), and laser ablation inductively-coupled plasma mass spectrometry (LA–ICP-MS)(Rice University). Sr–Nd–and Pb-isotopic compositions were measured for a subset of these samples via thermal ionization mass spectrometry (TIMS) at USGS (Denver) and Open University (Doe et al., 1982; Leeman et al., 1992; Bonnichsen et al., 2008; Leeman, unpublished data). Oxygen isotope ratios were measured at USGS (Denver) by standard BrF_5 extraction and are quoted as $\delta^{18}O_{VSMOW}$, i.e. relative to the Vienna standard mean ocean water [VSMOW] (for further analytical details on the oxygen isotope measurements see Boroughs et al., 2005). In some cases, our Sr–Nd-, Pb- or O isotope data are supplemented by published analyses for the same or equivalent samples (Hildreth et al., 1984, 1991; Boroughs et al., 2005). Three rhyolite samples (two with very low Sr concentrations), were analyzed for their Sr isotope ratios at the University of Leeds using a Thermo Finnigan *TRITON* TIMS instrument running in static mode. The total Sr blank was negligible (<100 pg) and the SRM 987 gave average $^{87}Sr/^{86}Sr$ of 0.710246 ($n=19$). Using isotope dilution techniques we also evaluated the Sr concentrations of the low Sr samples that were measured by LA–ICP-MS. It appears that the Sr concentrations analyzed by LA–ICP-MS are well within the values we obtain by isotope dilution TIMS (ID–TIMS): *6YC-146* (*Lava Creek rhyolite*): $Sr_{(LA–ICP-MS)}=4.9$ ppm; $Sr_{(ID–TIMS)}=6.2$ ppm; *8YC-396A* (*Crystal Springs flow rhyolite*) $Sr_{(LA–ICP-MS)}=4.5$ ppm; $Sr_{(ID–TIMS)}=4.1$ ppm; *I-556* (*Cougar Point Tuff V*): $Sr_{(LA–ICP-MS)}=18.1$ ppm; $Sr_{(ID–TIMS)}=21.2$ ppm.

Boron isotopic analyses of natural rhyolite glasses were made using multiple multiplier laser ablation inductively-coupled plasma mass spectrometry (MM-LA–ICP-MS) techniques developed at the Department of Terrestrial Magnetism of the Carnegie Institution of Washington (leRoux et al., 2004). Analyses were made on a Cetac LSX200 Nd-YAg frequency-quadrupled laser, operating at 266 nm, coupled to a VG Elemental Axiom double-focusing multi-collector ICP-MS. Laser spot sizes were 30 μm, with laser scan speeds of 10 μm/s and repetition rate of 20 Hz; typically, this method samples a trench that is ~1000 μm long and only a few μm deep. The NIST-612 glass standard was used to monitor instrumental drift, and B-specific isotope standards B-5 (basalt) and B-6 (rhyolite obsidian) were analyzed to monitor precision and accuracy. Final $\delta^{11}B$ values were referenced to $^{11}B/^{10}B$ value of 4.05003 for the NIST-951 B standard (Ishikawa and Tera, 1997; Ishikawa et al., 2001). Repeated runs of the B-5 and B-6 standards give $^{10}B/^{11}B$ of 4.0462 and 4.0355, respectively, almost identical to the literature $^{10}B/^{11}B$ for these samples (Tonarini et al., 2001; Gonfiantini et al., 2003). The measured 2σ precision was always better than 1‰ (the average of all unknown rhyolite glass analyses is ±0.3 ‰). Further details of the analytical technique used for B isotope measurements are provided in leRoux et al. (2004) and Tiepolo et al. (2006). In addition, we also report preliminary SIMS data for boron isotopic composition of the two primitive SRP basalts. These analyses were made on synthetic glasses prepared from the whole-rock powders following techniques described in leRoux et al. (2004). The SIMS data were collected at University of Heidelberg on a modified Cameca ims 3f ion microprobe (equipped with a primary beam mass filter), following methods and procedures described in Marschall et al. (2007).

Boron concentrations of most bulk samples were determined via prompt-gamma neutron activation (PGNA) with accuracy and precision better than 10% (cf. Leeman, 1988). To provide a consistent database for comparison with the in-situ B isotopic measurements, most samples were analyzed for major and for B and other trace elements via laser ablation ICP-MS using a ThermoFinnigan Element 2 mass spectrometer and a NewWave 213 nm laser ablation system at Rice University (cf. Agranier and Lee, 2007). For the basaltic samples, glasses were prepared for laser analysis by fusion in HF-cleaned and welded Pt capsules at 1500 °C; for the silicic rocks, natural glasses were analyzed. Data were collected in both low and medium resolution modes (with normalization to ^{40}Ca or ^{30}Si, respectively) to obtain optimal mass resolution for each element. Glass standards BHVO-2g (Hawaii basalt), BCR-2g (Columbia River basalt), and Bir-1g (Icelandic basalt) were used to calibrate all trace elements except for B. For B, these glass standards appear to have been contaminated during preparation, so PGNA data for three Oregon obsidians were used to calibrate B analyses by LA–ICP-MS. Overall accuracy and precision appear to be better than 5% for most elements reported. Analytical data are reported in Table 1.

5. Results

The data presented here (Table 1) are representative of a larger database for the region (cf. Leeman et al., 1992; Nash et al., 2006; McCurry et al. (2008)). Collectively, the available isotopic data demonstrate that a profound geochemical transition is associated with the boundary between cratonic North America and accreted oceanic terranes west of the WISZ (Oldow et al., 1989; Leeman et al., 1992; Camp and Ross, 2004). This is clearly seen in initial (i.e., calculated at age of eruption) Sr–Nd–Pb isotopic compositions of silicic volcanic rocks from a transect spanning from Yellowstone to Newberry volcano (Fig. 2). Nearly all of the studied rhyolites east of the WISZ transition zone (especially those from Yellowstone) have systematically elevated $^{87}Sr/^{86}Sr$, somewhat elevated $^{207}Pb/^{206}Pb$ and much lower $^{143}Nd/^{144}Nd$ than observed in rhyolites from eastern Oregon. Leeman et al. (1992) described similar patterns for Neogene basaltic rocks from this region. As seen in Fig. 2, most of the rhyolites east of WISZ are clearly distinctive from the associated basalts, and appear to have significant contributions from ancient, evolved continental crust. A notable exception is the Big Southern Butte (BSB) rhyolite (cf Fig. 2A,B). In contrast, rhyolites from Oregon are isotopically similar to their associated basalts, suggesting that they could be genetically related or that they are derived from relatively juvenile crustal sources with mantle-like isotopic compositions (e.g., oceanic crustal lithologies from the accreted terranes as outlined on Fig. 1). The observed lateral isotopic variations have been attributed to the juxtaposition of distinct crustal and mantle domains along an old truncated lithospheric boundary (Leeman et al., 1992). The presence of thicker and more evolved cratonic crust to the east also is likely to influence many aspects of magma generation and ascent. For example, it is inferred that stagnation of large volumes of basaltic magma in the cratonic crust resulted in extensive crustal melting and significantly larger volumes of silicic magma in that region compared to in areas west of the craton (Bonnichsen et al., 2008; Leeman et al., 2008).

There are also significant regional differences in major and trace element composition of the silicic volcanic rocks. For example, as seen in Fig. 3, the SRPY rhyolites have systematically lower Na_2O/K_2O and higher contents of Th and other lithophile elements (e.g., Rb, U, La, Nb; not shown) compared to those west of the WISZ (also cf. Streck and Grunder, 2007). The BSB rhyolite resembles main trend SRPY rhyolites in most respects, whereas the COM latite has Th and Na_2O/K_2O values similar to those for eastern Oregon rhyolites. Large distinctions similarly extend to B systematics (Fig. 4), except that B concentrations and enrichments with respect to other incompatible elements are antithetic to the lithophile elements. For example, B/Rb and B/Nb are

Table 1
Major element, trace element and isotope ratios of samples from the SRPY discussed in the text.

Suites	High Lava Plains, Oregon				Bruneau-Jarbidge center, SRP			Yellowstone center				Miscellaneous				SRP basalts	
Sample	M3-79	M3-86	M3-33	BOF*	I-556	I-841	I-459	6YC-143	9YC-496A	8YC-396A	OCB66-06	6YC-146	L74-23	69-20	BGF-2*	6YC-142	73L-64
Loc/Unit	Burns Butte dome	Egli Ridge dome	Squaw Rdge dome	Big Obs Flow, Newberry Caldera	Cougar Point Tuff V	Cougar Point Tuff VII	Cougar Point Tuff XV	Nez Perce flow (IC)	Canyon flow (IC)	Crystal Springs flow (EC)	Obsid Cliff flow (EC)	Lava Creek Tuff, mbr. B	Big Southern Butte	Devils Orchard flow, Craters of the Moon	Mono Craters	Gerritt basalt, Mesa Falls	Fissure basalt, Spencer Kilgore
Material	Obsidian	Obsidian	Obsidian	Obsidian	Vitric wr	Vitric wr	Vitric wr	Vitric wr	Vitric wr	Obsidian	Obsidian	Vitric wr	Obsidian	Obsidian	Obsidian	Basalt wr	Basalt wr
Age (my)	7.54	6.41	3.59	0.0013	12.07	11.81	10.50	0.15	0.48	0.07	0.17	0.64	0.30	0	Late Holocene	~0.2	~0.5
N Lat.	43.57	43.38	43.53	43.69	41.90	41.93	42.06	44.55	44.74	44.85	44.83	44.13	43.41	43.43	37.52	44.19	44.21
W Long.	119.14	119.85	120.78	121.23	115.30	115.42	115.64	110.83	110.48	110.72	110.73	110.82	113.04	113.55	119.02	111.33	111.69
SiO_2**	74.99	75.66	76.30	73.18	76.16	73.29	73.85	76.93	75.52	76.86	77.08	76.89	75.90	62.06	71.37	47.77	48.68
TiO2	0.19	0.13	0.13	0.21	0.23	0.49	0.42	0.09	0.35	0.09	0.08	0.04	0.11	0.77	0.29	1.14	1.21
Al2O3	13.55	13.68	12.95	14.46	12.46	13.01	12.87	11.90	12.84	12.19	12.10	12.10	12.47	14.75	15.61	16.98	14.80
FeO*	1.40	0.96	1.51	2.07	1.68	2.99	2.76	1.47	2.06	1.27	1.26	1.31	1.84	9.28	1.82	10.57	10.57
MnO					0.03	0.05	0.05	0.00	0.04	0.03	0.03	0.00	0.00	0.23	0.04	0.18	0.18
MgO	0.12	0.07	0.04	0.20	0.21	0.42	0.50	0.05	0.17	0.04	0.03	0.02	0.04	0.41	0.27	9.14	10.71
CaO	0.59	0.53	0.68	1.00	0.56	1.35	1.40	0.49	0.89	0.49	0.45	0.53	0.48	3.20	1.14	11.47	11.03
Na2O	4.22	4.33	4.39	4.82	2.47	2.52	2.90	3.58	2.70	3.99	3.93	3.78	4.40	4.55	3.57	2.35	2.15
K2O	4.92	4.63	3.99	4.01	6.16	5.78	5.18	5.47	5.40	5.04	5.05	5.33	4.74	4.50	5.85	0.24	0.36
P2O5	0.02	0.02	0.01	0.05	0.03	0.09	0.06	0.01	0.02	0.00	0.00	0.00	0.02	0.25	0.04	0.16	0.28
Na/K	0.86	0.94	1.10	1.20	0.40	0.44	0.56	0.65	0.50	0.79	0.78	0.71	0.93	1.01	0.61	9.79	5.92
ICP-MS data***	Rice LA	Rice LA	Rice LA	Rice LA	Rice LA	Rice LA	Rice LA	Rice LA	Rice LA	Rice LA	Rice LA	Rice LA	Rice LA	Rice LA	Rice LA	WSU solution	WSU solution
Cs	2.78	4.73	4.58	6.38	4.03	4.92	4.16	3.75	4.80	5.15	4.20	5.52	4.54	1.19	7.72		0.12
Li	31.1	44.4	55.0	40.1	31.6	29.7	27.5	41.2	-	74.6	71.3	49.6	116.7	34.4	57.4	4.2	10.2
Ba	576.8	1451.1	1009.6	943.9	493.8	1307.2	998.1	147.2	975.0	42.1	39.2	129.1	2.6	4114.7	804.2	130	186
Rb	102.8	109.3	120.8	169.2	207.3	253.5	191.8	177.9	179.0	230.5	200.2	314.1	277.9	89.4	126.6	5	6.7
Sr	20.5	35.4	39.7	45.9	18.1 ^^	41.9	32.0	7.0	84.0	4.5 ^^	2.6	4.9 ^^	0.2	216.7	99.0	189	174
Y	31.1	33.8	48.3	53.3	51.0	51.8	50.0	48.7	65.0	62.5	77.3	99.7	180.7	117.3	14.3	21	23.4
Zr	252.7	144.0	252.0	493.0	308.9	489.8	405.6	228.7	376.0	178.8	219.6	298.6	351.7	2106.8	203.2	76	109
Nb	27.6	15.6	14.1	34.5	43.3	50.4	41.6	45.7	51.0	41.5	39.3	104.3	274.5	126.3	6.7	5	10.1
Th	8.70	6.76	8.71	13.94	34.62	36.03	35.20	23.85	22.90	30.57	30.17	35.19	20.75	10.45	10.26	0.6	0.72
U	3.83	3.18	4.09	6.16	8.99	9.26	9.27	6.55	5.30	8.46	6.28	10.10	11.07	2.89	4.63	0.14	0.23
Pb	14.53	21.53	16.39	22.04	29.24	32.35	30.03	26.41	28.00	38.39	28.86	45.44	86.46	37.36	14.32	1.48	1.97
Zn	42	49	79	55	63	52	59	69	72	89	66	88	329	276	34	71	76.0
V	3.4	1.5	1.9	1.7	0.6	1.7	1.0	0.2		0.9	0.1	0.1	0.1	0.2	13.4	241.0	245

Suites	High Lava Plains, Oregon				Bruneau-Jarbidge center, SRP			Yellowstone center				Miscellaneous				SRP basalts	
Sample	M3-79	M3-86	M3-33	BOF*	I-556	I-841	I-459	6YC-143	9YC-496A	8YC-396A	OCB66-06	6YC-146	L74-23	69-20	BGF-2*	6YC-142	73L-64
Loc/Unit	Burns Butte dome	Egli Ridge dome	Squaw Rdge dome	Big Obs Flow, Newberry Caldera	Cougar Point Tuff V	Cougar Point Tuff VII	Cougar Point Tuff XV	Nez Perce flow (IC)	Canyon flow (IC)	Crystal Springs flow (EC)	Obsid Cliff flow (EC)	Lava Creek Tuff, mbr. B	Big Southern Butte	Devils Orchard flow, Craters of the Moon	Mono Craters	Gerritt basalt, Mesa Falls	Fissure basalt, Spencer Kilgore
ICP-MS data***	Rice LA	Rice LA	Rice LA	Rice LA	Rice LA	Rice LA	Rice LA	Rice LA	Rice LA	Rice LA	Rice LA	Rice LA	Rice LA	Rice LA	Rice LA	WSU solution	WSU solution
La	31.0	27.3	24.9	37.7	81.1	79.7	75.5	66.7	80.0	55.0	56.4	99.4	60.5	141.0	15.2	6.0	11.3
Ce	64.6	58.0	57.5	82.6	157.3	157.1	155.6	138.5	146.0	115.2	103.9	209.7	128.3	211.3	32.1	14.0	22.4
Pr	6.35	5.86	6.11	8.44	15.28	15.11	14.44	13.26		11.44	11.78	20.47	12.54	32.28	3.39		
Nd	23.48	23.08	26.22	33.64	54.84	54.69	50.04	47.43	73.00	42.97	47.10	76.52	43.53	123.36	13.01		12.8
Sm	4.72	4.83	6.37	7.26	10.24	10.50	9.49	9.24	12.90	9.99	11.23	15.95	12.16	23.29	2.77	2.7	3.5
Eu	0.33	0.56	0.70	0.96	0.59	0.87	0.73	0.39	1.73	0.13	0.12	0.54	0.24	6.62	0.43	1.06	1.26
Gd	4.71	5.05	6.78	7.52	10.19	10.57	9.47	9.61		10.80	12.97	16.34	17.47	23.57	2.84		3.74
Tb	0.76	0.81	1.11	1.23	1.55	1.61	1.44	1.48	1.60	1.80	2.14	2.64	3.52	3.55	0.42	0.55	0.68
Dy	5.36	5.60	7.71	8.49	10.61	10.00	9.72	9.69		11.82	14.34	17.21	28.70	21.96	2.74		
Ho	1.12	1.18	1.63	1.85	2.07	2.07	2.00	1.94		2.33	2.93	3.45	6.49	4.39	0.55		
Er	3.41	3.54	4.74	5.61	5.79	5.92	5.60	5.54		6.47	8.21	10.01	19.75	13.18	1.62		
Tm																	0.37
Yb	3.88	3.93	5.09	6.37	5.55	5.68	5.43	5.25	6.30	6.07	7.57	9.84	20.86	13.20	1.74	2.05	2.25
Lu	0.63	0.63	0.78	0.99	0.85	0.80	0.79	0.79	0.85	0.89	1.11	1.38	3.04	2.04	0.28	0.34	0.35
Sc	4.0	4.4	4.1	6.0	3.3	5.5	3.8	2.7	r.85	1.7	2.0	1.7	0.7	24.4	4.5	37.0	36.7
Co	0.9	0.5	0.3	1.2	0.5	1.0	0.8	0.3		0.4	0.3	0.4	0.1	2.1	1.7	53	44
Hf	7.34	5.10	6.96	11.15	11.01	14.97	12.52	9.31	10.50	9.64	10.93	10.27	19.34	45.27	5.71	1.60	2.54
Ta	1.88	1.16	1.11	2.42	2.96	3.23	2.86	3.10	3.71	3.07	3.03	6.80	17.82	6.58	0.67	0.40	0.56
B	20.5	61.6	23.0	16.7	11.6	10.9	11.2	10.9	10.0	12.5	12.8	11.0	22.4	11.1	17.7		
B (PGNA)	21	60	24	20.5	12	11	11	11	10	13	13	12.0	22	11		1.1	1.5
δ^{11}B	−0.8	−2.2	−2.5	−3.1	−5.6	−8.9	−8.6		−8.5	−7.8	−7.4		−6.1	−2.1	0.4	[a]1.5	[a]−4.7
±	0.5	0.3	0.4	0.3	0.2	0.3	0.2	–	0.3	0.2	0.3	–	0.2	0.4	0.4	3.2	3.9
$Sr^{87}/^{86}Sr$	0.70550	0.70470	0.70490	0.70350	0.71556 ^	0.71154	0.71036	0.71000	0.71603	0.71059 ^	0.71505	0.71101 ^	0.72493	0.71040	–	0.70614	0.70596
$Nd^{143}/^{144}Nd$	–	–	–	0.512955	–	0.512191	0.512216	–	0.512165	–	0.511956	–	0.512326	0.512257	–	0.512460	0.512375
εNd	–	–	–	6.18	–	−8.72	−8.23	–	−9.23	–	−13.30	–	−6.09	−7.43	–	−3.47	−5.13
δ^{18}O	4.4	7.6	7.9	–	2.9	0.2	1.0	3.4	0.2	7.1	4.7	5.0	6.0	7.1	–	5.9	–
$^{206}Pb/^{204}Pb$	18.836	18.777	18.927	19.048	–	–	–	17.622	17.806	–	17.137	17.299	17.622	17.806	–	17.310	17.396
$^{207}Pb/^{204}Pb$	15.602	15.607	15.610	15.639	–	–	–	15.590	15.633	–	15.538	15.544	15.590	15.596	–	15.520	15.482
$^{208}Pb/^{204}Pb$	38.597	38.479	38.596	38.689	–	–	–	38.323	38.348	–	38.289	38.415	38.323	38.434	–	38.240	38.027
$^{207}Pb/^{206}Pb$	0.828	0.831	0.825	0.821	–	–	–	0.885	0.878	–	0.907	0.899	0.885	0.876	–	0.897	0.890
B/Nb	0.7	3.9	1.6	0.5	0.3	0.2	0.3	0.2	0.2	0.3	0.3	0.1	0.1	0.1	2.6	0.2	0.1
B/Rb	0.20	0.56	0.19	0.10	0.06	0.04	0.06	0.06	0.06	0.05	0.06	0.04	0.08	0.12	0.14	0.00	0.00

Notes: Major elements are for whole rock (wr) samples. ICP trace elements are for natural glasses except for sample 9YC–496A and the basalts; for these wr data are presented.
*Sample from J. Castro (Smithsonian Institution).
** = All major el. data in wt.%.
*** = All ICP-MS data in ppm.
^Analyzed on TRITON TIMS at Univ. Leeds.
^^ = Re-analyzed by isotope dilution on TRITON TIMS at Univ. Leeds (see analytical techniques section).
[a] Preliminary SIMS data.

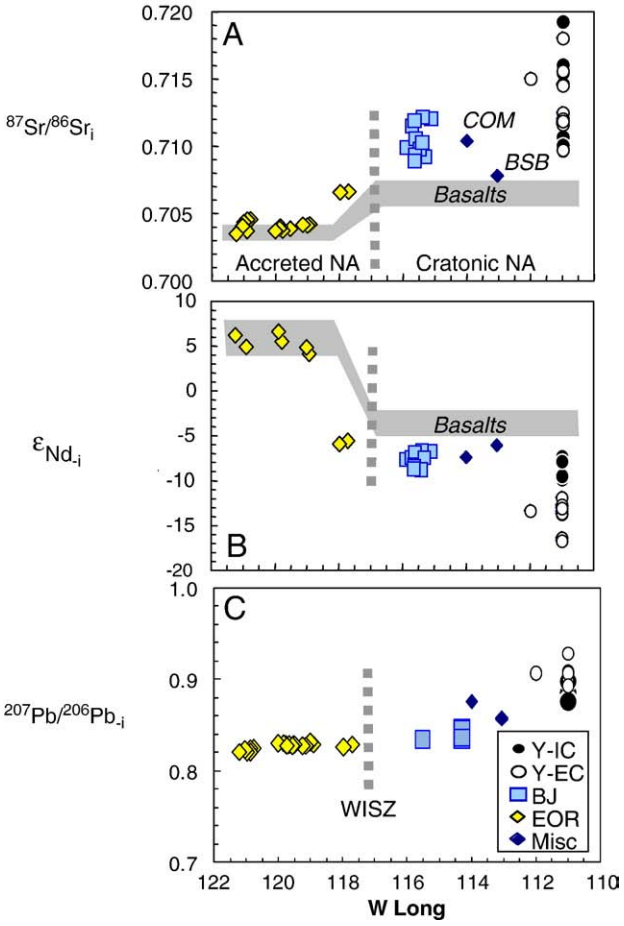

Fig. 2. East–west variation in initial (i.e., at time of eruption) Sr, Nd, and Pb isotopic compositions of silicic volcanic rocks in the studied traverse. Samples are distinguished as follows: Yellowstone intracaldera (Y-IC) and extracaldera (Y-EC) rhyolites, Bruneau-Jarbidge (BJ) rhyolites, eastern Oregon (EOR) rhyolites; young Craters of the Moon (COM) latite and Big Southern Butte (BSB) rhyolite are plotted as miscellaneous (Misc) samples. Vertical dashed line shows position of the western Idaho suture zone (WISZ), which we infer to mark the western boundary of the North American craton. Gray shading indicates the compositional range for Neogene basalts from the HLP and SRP. Coincidence of the profound isotopic boundaries with the WISZ is taken to signify a dramatic lateral variation in magma source compositions across this tectonic boundary — both in the crust and in the mantle (cf. Leeman et al., 1992). These data are consistent with involvement of old isotopically evolved source material to the east and relatively juvenile sources to the west. With regard to Sr and Nd compositions, most rhyolites to the east (except perhaps BSB) are isotopically distinct from the associated basalts. In contrast, to the west most rhyolites overlap the isotopic range of the associated basalts — which in turn are similar to many oceanic basalts.

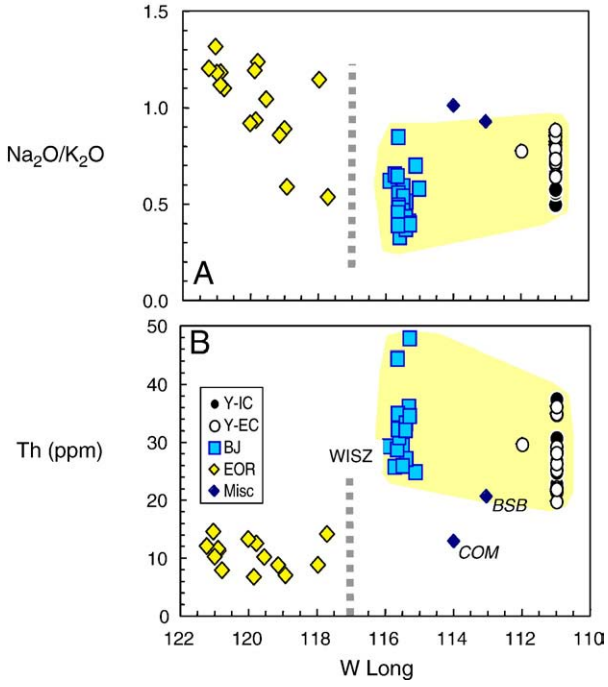

Fig. 3. East–west variation in selected compositional parameters in silicic volcanic rocks from the studied traverse. SRPY main trend rhyolites erupted from vents on cratonic North America (shaded fields group samples from Yellowstone and Bruneau-Jarbidge) are systematically enriched in K_2O relative to Na_2O and in Th (also Rb, Nb, La; not shown) compared to rhyolites erupted from the area underlain by accreted oceanic terranes east of the WISZ. These data also reflect involvement of evolved cratonic crust in rhyolites to the east and relatively primitive crust to the west. Symbols as in Fig. 2.

significantly lower in SRPY rhyolites compared with ones from eastern Oregon. Boron isotopic composition is also distinct for these areas, with low $\delta^{11}B$ values (−5 to −10‰) in SRPY rhyolites. The COM latite has a distinctly heavier $\delta^{11}B$ (−2‰). Eastern Oregon rhyolites also have heavier $\delta^{11}B$ values (0 to −3‰) that overlap the range observed for the Cascades volcanic front (Fig. 4A). These data are consistent with the radiogenic isotope data in suggesting that on- and off-craton rhyolites have distinctive sources. Moreover, B is decoupled from other incompatible elements.

6. Discussion

Before discussing the significance of our results, it is first necessary to determine if the B relations reflect primary magmatic processes or the influence of shallow crustal processes. Direct comparison of $\delta^{18}O$ with B isotopic composition and elemental enrichment is shown in Fig. 5. The near constancy of $\delta^{11}B$ in SRPY rhyolites with highly

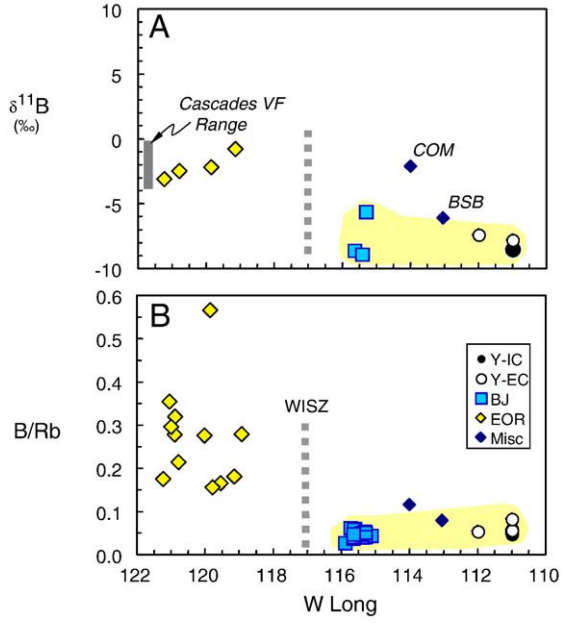

Fig. 4. East–west variation in boron systematics in silicic volcanic rocks from the studied traverse. (A) Boron isotopic composition ($\delta^{11}B$) is systematically lighter to the east (with exception of COM latite) compared to eastern Oregon rhyolites; the latter overlap with compositions of basaltic to dacitic lavas from the Cascades volcanic front (VF). (B) B/Rb also is systematically lower in all silicic volcanic rocks from the cratonic region; this reflects an antithetic variation of B (enriched to the west) with respect to other incompatible elements like Rb, Th, Nb, La (all enriched to the east). In other words, B is decoupled from these other elements. Symbols as in Fig. 2.

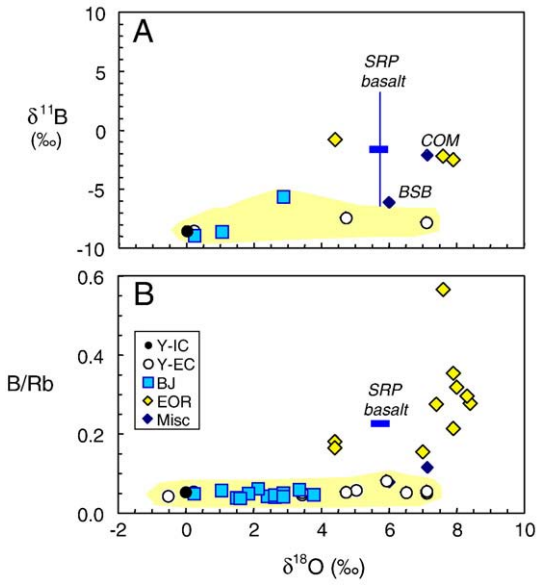

Fig. 5. Comparison of B systematics with oxygen isotopic composition. Most eastern Oregon rhyolites have relatively normal $\delta^{18}O$ values (+7 to +9‰), with slightly lower values (down to +4‰) in two ignimbrites. SRPY rhyolites have much more variable $\delta^{18}O$ with exceptionally low values in all BJ samples and in certain post-caldera rhyolites from Yellowstone. In contrast, $\delta^{11}B$ (A) and B/Rb (B) display very small variability in SRPY rhyolites and are essentially decoupled from $\delta^{18}O$. Thus, processes that cause large variation in $\delta^{18}O$ seem to have little effect on B geochemistry. Also note that SRP basalts have systematically higher B/Rb than associated rhyolites; despite large analytical uncertainty for the basalt data, this appears to be the case for $\delta^{11}B$ as well.

variable $\delta^{18}O$ shows that these parameters are uncorrelated, and suggests that the processes that caused the wide range in oxygen isotopic composition have little effect on the B systematics. Our fresh rhyolite glasses from Yellowstone and Bruneau-Jarbidge have similar $\delta^{11}B$ values (−7 to −9 ‰, with one value of −5.6 ‰), and these are slightly lower than the one fresh glass analysis (−5.5 ‰) of Palmer and Sturchio (1990). Because their analysis (−9.7 ‰) of a hydrothermally altered part of the same lava is similar to our data for fresh glasses, it appears that isotopic fractionation associated with hydrothermal alteration is negligible. Also, B/Rb in SRPY rhyolites (Table 1) is remarkably uniform and uncorrelated with $\delta^{18}O$ variations (Fig. 5). From these data, it appears that caldera hydrothermal processes that shape the low $\delta^{18}O$ compositions in many SRPY rhyolites (Bindeman and Valley, 2000, 2001b) are not responsible for the observed strong B-depletion and low $\delta^{11}B$ values.

Fig. 5 also compares the rhyolite data to those available for primitive SRP basalts (Table 1). Although not precisely determined, average $\delta^{11}B$ (ca. −2 ‰) for the basalts appears to be higher than that for SRPY rhyolites and similar to that for the COM latite. However, the basalts clearly have higher B/Rb than any of the SRPY silicic volcanic rocks, and this observation suggests that SRPY rhyolites are unlikely to be derived from parental magmas similar to SRP basalts. At present, we have insufficient data to evaluate such relations for E. Oregon rhyolites.

It is instructive to examine variations of B and other incompatible elements as a function of differentiation; for this purpose we consider how B, Th, B/Rb, and Th/Ta vary with SiO_2 content (Fig. 6). The trace element contents display distinct trends for each subset of samples. B tends to increase with SiO_2, following distinct paths for SRPY and HLP samples. Thorium contents define more complex patterns. Yellowstone rhyolites show a two-fold range in Th at near constant SiO_2, whereas BJ rhyolites define a coherent positive correlation. However, unlike expected differentiation trends, both thorium and SiO_2 actually decrease over time in the BJ samples. This array likely reflects mixing of high-silica rhyolite with more mafic or intermediate composition magmas. Leeman et al. (2008) suggest that the lower SiO_2 magmatic end-members could be partial melts of mafic intrusive rocks or basaltic differentiation products. The COM latite illustrates that suitable mixing components are present beneath the SRPY province. Thorium appears to be negatively correlated with SiO_2 in the Oregon samples.

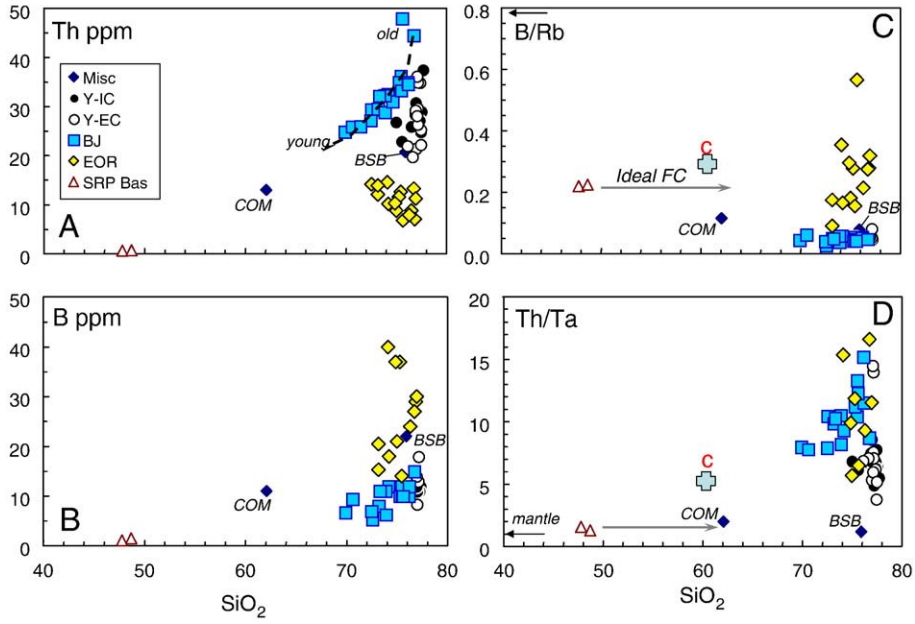

Fig. 6. Variation in selected trace element concentrations and ratios with SiO_2 (wt.%) in silicic volcanic rocks from the studied traverse and in representative SRP basalts (Table 1). (A) Thorium; (B) Boron (C) B/Rb and (D) Th/Ta. The BJ data define a striking positive Th-SiO_2 correlation, but note this trend is anticorrelated with age. Yellowstone rhyolites display a two-fold range in Th at near constant SiO_2. The EOR samples appear to define a weak negative Th-SiO_2 correlation. There is a good positive correlation between the SiO_2 and B concentrations of BJ. B/Rb (C) and Th/Ta (D) ratios display considerable variability whereas they should be relatively constant in closed system fractional crystallization scenarios (cf. horizontal arrows). Also, note that SRPY rhyolites have B/Rb significantly lower than average continental crust [C] (Leeman et al., 1992; Rudnick and Gao, 2004), but within the expected range for granulitic lower crust. B/Rb in these rhyolites is also lower than in associated basalts. In contrast, Th/Ta ratios bracket expected crustal values. All SRPY rhyolites except BSB (and COM latite) have significantly higher Th/Ta than associated basalts.

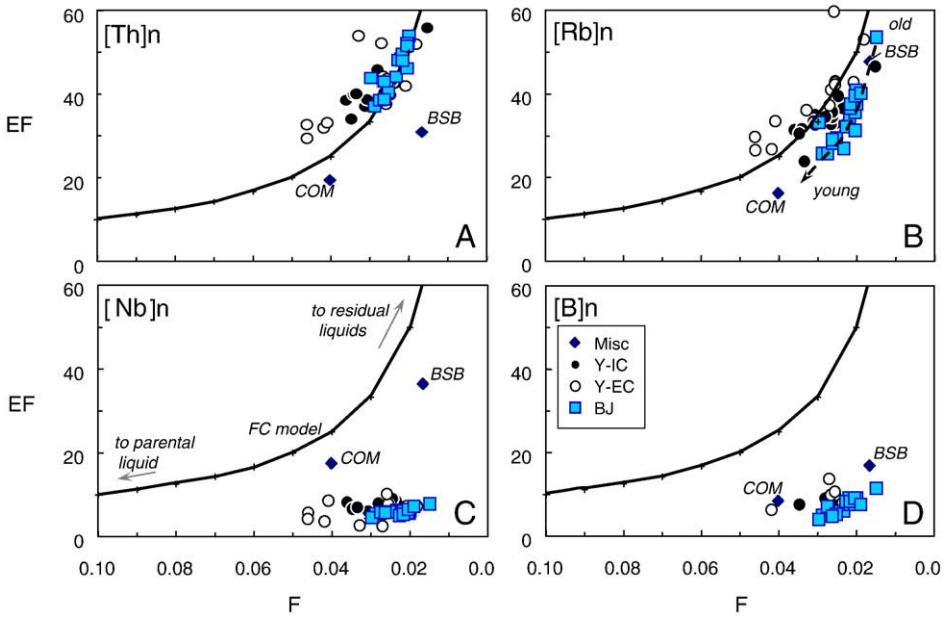

Fig. 7. Evaluation of fractional crystallization (FC) processes. Assuming a basaltic parent for SRPY rhyolites, degree of crystallization is predicted based on the enrichment factor (EF) for uranium. F, the fraction of melt remaining for a given sample, ideally is proportional to the inverse enrichment factor as calculated from U concentration in rhyolite divided by that in average basalt. If the rocks are related by closed system FC, enrichment factors for similarly incompatible elements (e.g., Th, Rb, Nb, B) should closely parallel that for U and plot along ideal FC curves (see text). This diagram demonstrates that, while the expected relations approximately hold for Th and Rb, they do not for Nb and B. Also, as noted earlier, BJ samples define the equivalent of a reverse fractionation trend, becoming less evolved over time. Arrows on left-hand side of panels C and D indicate typical mantle ratios (Ryan et al., 1996; Willbold and Stracke, 2007).

Because element concentrations depend strongly on both the nature and extent of magmatic differentiation processes, it is more informative to consider ratios between elements of similar incompatibility in silicate melts. For SRPY rhyolites, B/Rb ratios are remain nearly constant over the full range in SiO_2, and they are lower than those in the COM latite or SRP basalts. Differentiation of such basalts ideally would produce derivative liquids with constant (or slightly increasing, if sanidine was among the crystallizing phases) B/Rb and certainly ratios that are higher than those observed for the rhyolites. Likewise, this process would produce derivative liquids having similar Th/Ta to that (~1) in the basalts, yet SRPY rhyolites have significantly higher Th/Ta ratios that reflect their crustal precursors.

Finally, we compare enrichment factors for several highly incompatible elements in Fig. 7. Assuming that individual SRPY rhyolites are derived from a common basaltic parental magma, enrichment factors can be obtained by normalizing the concentration in a given rhyolite to that of the average basalt. The fraction (F) of liquid remaining in this scenario is given as the inverse of the enrichment factor, and F was approximated using normalized U contents. These approximations of F are in turn compared with enrichment factors (EF) based on Th, Rb, Nb, and B contents, and with an ideal FC model (where $F = 1/EF = C_B/C_R$; where C_B and C_R are concentrations of an element in basalt and rhyolite, respectively; and bulk solid/liquid partition coefficients are assumed to approach zero). While SRPY data for Th and Rb fit ideal fractionation curves very well, the data for Nb and B do not. Misfits might be partly rationalized by allowing that there is some variability in parental magmas, but this clearly cannot explain the fact that the measured Nb and B contents in the rhyolites are considerably lower than predicted by the model. Moreover, '*F*' appears to decrease further back in time for the BJ suite, which is opposite expectation for ideal fractionation trends (e.g., Fig. 7B).

The conclusion from this and from foregoing trace element constraints is that it is virtually impossible to reconcile the low B contents of SRPY rhyolites with fractional crystallization scenarios beginning with the associated basalts as parental magmas. If FC is involved, it must be accompanied by other processes such as open system mixing of different magmatic components. However, to get the observed low B contents and relative depletion of B with respect to other incompatible elements, it is more plausible to invoke B-depletion in the crustal magma source(s). As discussed by Shaw et al. (1988), Nabelek et al. (1990) and Leeman et al. (1992), this is a predicted consequence of increasing metamorphic grade in the lower to middle crust. In fact, Archean crustal xenoliths from SRP lavas exhibit extreme B-depletion with concentrations sometimes well below 1 ppm (Leeman et al., 1985, 1992). Such rocks need not reside physically in the lower crust today, but they were likely metamorphosed at such depths during their long-lasting habitation in the

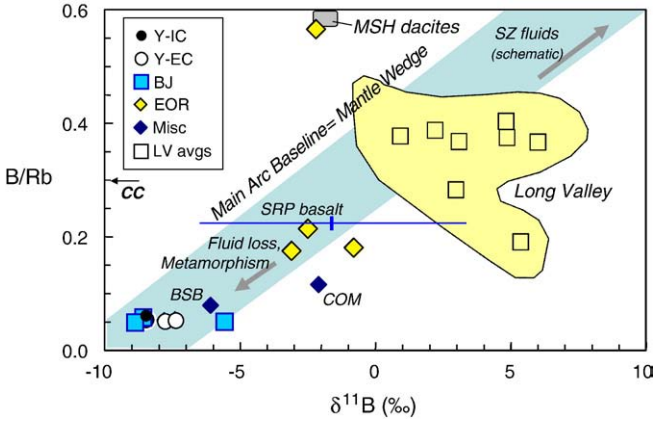

Fig. 8. Overview of the B and B isotope systematics. Symbols as in previous diagrams but with data added for Long Valley (LV) rhyolites (Schmitt and Simon, 2004), SRP basalts (Table 1), and Mount St. Helens (MSH) dacites (Leeman et al., 2004). Shaded field (yellow) shows range of individual SIMS analyses for LV melt inclusions. Linear field (gray) shows main trend for global volcanic arc magma sources (Ishikawa and Tera, 1997; Tonarini et al., 2001; Ishikawa et al., 2001; Schmitt et al., 2002; Savov et al., 2007b). The arrow pointing toward subduction zone (SZ) fluids is based on data and discussions in Ishikawa and Tera (1997) and Savov et al. (2004, 2007a). Arrow labeled CC denotes the approximate B/Rb ratio expected for bulk continental crust ($\delta^{11}B$ composition is likely variable).

crust. Another consequence of metamorphism is that devolatilization processes can selectively mobilize ^{11}B in the fluid phase leaving a B-poor refractory residue with lighter $\delta^{11}B$ than the original protolith (Palmer and Swihart, 1996; Leeman and Sisson, 1996; Marschall et al., 2008). Unfortunately, because of very low B contents, there are hardly any direct measurements of B isotopic composition for lower crustal rocks.

Such effects can be appreciated in the context of regional variations in B systematics (Fig. 8). This diagram shows data for the studied transect, for the Cascades (Leeman et al., 2004) and Long Valley (Schmitt and Simon, 2004) areas, as well as a general array expected for the mantle wedge as deduced from global studies of arc volcanic rocks having minimal or 'baseline' B contents (Ishikawa and Tera, 1997; Tonarini et al., 2001; Ishikawa et al., 2001; Savov et al., 2007b; Leeman and Tonarini, unpublished data). Samples with $\delta^{11}B>0$ ‰ are rare in intraplate settings (OIBs, MORBs) (Chaussidon and Jambon, 1994), so the bulk of the mantle is probably restricted to lower values. Ingress of ^{11}B-fluids from subducted slabs commonly is invoked to explain higher $\delta^{11}B$ values like those in the Long Valley rhyolites, or in samples that plot above the array (Mt. St. Helens [MSH], some HLP rhyolites). In most arcs there are lavas that show upward excursions from this array owing to variable inputs of B-rich fluids. However, the bulk of our rhyolites have $\delta^{11}B<0$ ‰. There are two logical explanations for this range. Although they could conceivably be derived from basaltic magmas that originated from mantle sources with compositions along the baseline array (Chaussidon and Marty, 1995; Ryan et al., 1996), we have shown that this is unlikely at least for the SRPY rhyolites. For example, the discrepancy in B/Rb and $\delta^{11}B$ between associated basalts and rhyolites from the SRPY province is inconsistent with a genetic relation between the two magma types. The second, and more favored, hypothesis is that SRPY rhyolites represent melts of refractory crust from which ^{11}B has been selectively removed as a consequence of intense metamorphism. We propose that the SRPY rhyolite data provide a plausible estimate for the B isotopic composition of the lower crust beneath this region.

7. Conclusions

This study documents systematic lateral variations in the isotopic and elemental compositions of silicic magmas from the NW USA. In particular, there are significant enrichments of B and higher $\delta^{11}B$ values in rhyolites associated with accreted oceanic terranes from eastern Oregon, and lower B and $\delta^{11}B$ values in rhyolites associated with the Archean craton underlying much of southern Idaho. B enrichment is anticorrelated with abundances of lithophile trace elements, demonstrating that B systematics are decoupled by processes that can selectively remove only B. Because aqueous fluids can effectively mobilize B, it is likely that they are responsible for the inferred decoupling. The absence of correlations between B, $\delta^{11}B$, and $\delta^{18}O$ in the rhyolites suggests that shallow crustal hydrothermal processes have little influence on B systematics of these rocks. Likewise, various geochemical relations rule out differentiation of the rhyolites from associated basalts, and thus B systematics are unlikely to be inherited from the mantle. The most plausible option is that B systematics of the rhyolites reflect the evolution of crustal sources that melt to produce these magmas. We suggest that intense (granulite grade) metamorphism during Archean time dehydrated portions of the cratonic crust and selectively removed B and ^{11}B (lower $\delta^{11}B$) to produce appropriate source materials. In the Oregon rhyolites, elevated B contents and selective enrichments of B with respect to other incompatible elements are also difficult to explain via direct fractionation of basaltic magmas. For example, elemental ratios between B and other incompatible elements are too variable to be consistent with this process. It is likely that they too are derived by crustal melting in response to basaltic intrusions. However, sources for the Oregon rhyolites must be juvenile to explain their oceanic-like Sr–Nd–Pb compositions.

Acknowledgements

The mass spectrometry support of Tim Mock was critical for the success of the B isotope study. Much of the radiogenic and some of the oxygen isotope work reported here was completed by WPL using facilities at the USGS (Denver) and Open University (Milton Keynes, UK). Bruce Doe, Carl Hedge, Joe Whelen, Andy Gledhill, Martin Menzies, and Peter Van Calsteren are thanked for their support during those visits. IS would like to thank Thomas Ludwig (Heidelberg University) for the preliminary B isotope data. We thank R. L. Christiansen, J. Obradovich, B. Bonnichsen, Norm MacLeod, Jon Castro and Todd Feeley for supplying some of the samples used in this study. Formal journal reviews by Mary Reid, Peter Larson, Henrietta Cathey and Ian Ridley, as well as the guest editor Lisa Morgan helped us to clarify the SRP-Yellowstone petrology and geochemistry. WPL acknowledges support from the National Science Foundation for providing time to complete this research. IS acknowledges support during his postdoctoral stay at the Carnegie Institution of Washington, Department of Terrestrial Magnetism (DTM).

References

Agranier, A., Lee, C.T.A., 2007. Quantifying trace element disequilibria in mantle xenoliths and abyssal peridotites. Earth and Planetary Science Letters 257, 290–298.
Annen, C., Sparks, R.S.J., 2002. Effects of repetitive emplacement of basaltic intrusions on thermal evolution and melt generation in the crust. Earth and Planetary Science Letters 203, 937–955.
Annen, C., Blundy, J.D., Sparks, R.S.J., 2006. The Genesis of Calcalkaline Intermediate and Silicic Magmas in Deep Crustal Hot Zones. Journal of Petrology 47, 505–539.
Bacon, C.R., Adami, L.H., Lanphere, M.A., 1989. Direct evidence for the origin of low-$\delta^{18}O$ silicic magmas: Quenched samples of a magma chamber's partially-fused granitoid walls, Crater Lake, Oregon. Earth and Planetary Science Letters 96, 199–208.
Bindeman, I.N., Valley, J.W., 2000. The formation of low-d^{18}O rhyolites after caldera collapse at Yellowstone. Geology 28, 719–722.
Bindeman, I.N., Valley, J.W., 2001a. Low-$\delta^{18}O$ rhyolites from Yellowstone: Magmatic evolution based on analyses of zircons and individual phenocrysts. Journal of Petrology 42, 1491–1517.
Bindeman, I.N., Valley, J.W., 2001b. Post-caldera volcanism: In situ measurement of U–Pb age and oxygen isotope ratio in Pleistocene zircons from Yellowstone caldera. Earth and Planetary Science Letters 189, 197–206.
Bonnichsen, B., Leeman, W.P., Honjo, N., McIntosh, W.C., Godchaux, M.M., 2008. Miocene silicic volcanism in southwestern Idaho: geochronology, geochemistry, and evolution of the central Snake River Plain. Bulletin of Volcanology 70. doi:10.1007/s00445-007-0141-6.
Boroughs, S., Wolff, J., Bonnichsen, B., Godchaux, M., Larson, P., 2005. Large volume, low-$\delta^{18}O$ rhyolites of the central Snake River Plain, Idaho, USA. Geology 33, 821–824.
Boschi, C., Dini, A., Früh-Green, G.L., Kelley, D.S., 2008. Isotopic and element exchange during serpentinization and metasomatism at the Atlantis Massif (MAR 30°N): Insights from B and Sr isotope data. Geochimica et Cosmochimica Acta 72, 1801–1823.
Camp, V.E., Ross, M.E., 2004. Mantle dynamics and genesis of mafic magmatism in the intermontane Pacific Northwest. Journal of Geophysical Research 109, B08204. doi:10.1029/2003JB002838.
Castro, J.M., Mercer, C., 2004. Microlite textures and volatile contents of obsidian from the Inyo Volcanic Chain, California. Geophysical Research Letters 31, L18605. doi:10.1029/2004GL020489.
Chaussidon, M., Jambon, A., 1994. Boron content and isotopic composition of oceanic basalts; geochemical and cosmochemical implications. Earth and Planetary Science Letters 121, 277–291.
Chaussidon, M., Marty, B., 1995. Primitive boron isotope composition of the mantle. Science 269, 383–386.
Doe, B.R., Leeman, W.P., Christiansen, R.L., Hedge, C.E., 1982. Lead and strontium isotopes and related trace elements as genetic tracers in the Upper Cenozoic rhyolite–basalt association of the Yellowstone Plateau volcanic field. Journal of Geophysical Research 87, 4785–4806.
Draper, D.S., 1991. Late Cenozoic bimodal magmatism in the northern Basin and Range province of southeastern Oregon. Journal of Volcanology and Geothermal Research 47, 299–328.
Gonfiantini, R., Tonarini, S., Adorni-Braccesi, A., Al-Ammar, A.S., Astner, M., Bächler, S., Barnes, R.M., Bassett, R.L., Cocherie, A., Deyhle, A., Dini, A., Ferrara, G., Gaillardet, J., Grimm, J., Guerrot, C., Krähenbühl, U., Layne, G., Lemarchand, D., Meixner, A., Northington, D., Pennisi, M., Reitznerová, E., Rodushkin, I., Sugiura, N., Surberg, R., Tonn, S., Wiedenbeck, M., Wunderli, S., Xiao, Y., Zack, T., 2003. Intercomparison of boron isotope and concentration measurements. Part II: Evaluation of results. Geostandard Newsletters 27, 41–57.

Hervig, R.L., Moore, M., Williams, L.B., Peacock, S.M., Holloway, J.R., Roggensack, K., 2002. Isotopic and elemental partitioning of boron between hydrous fluid and silicate melt. American Mineralogist 87, 769–774.
Hildreth, W., Christiansen, R.L., O'Neil, J.R., 1984. Catastrophic isotopic modification of rhyolitic magma at times of caldera subsidence, Yellowstone Plateau volcanic field. Journal of Geophysical Research 89, 8339–8369.
Hildreth, W., Halliday, A.N., Christiansen, R.L., 1991. Isotopic and chemical evidence concerning the genesis and contamination of basaltic and rhyolitic magma beneath Yellowstone Plateau volcanic field. Journal of Petrology 32, 63–138.
Ishikawa, T., Nakamura, E., 1993. Boron isotope systematics of marine sediments. Earth and Planetary Science Letters 117, 567–580.
Ishikawa, T., Tera, F., 1997. Source, composition and distribution of fluid in the Kurile mantle wedge: constraints from across-arc variations of B/Nb and B isotopes. Earth and Planetary Science Letters 152, 123–138.
Ishikawa, T., Tera, F., Nakazawa, T., 2001. Boron isotope and trace element systematics of the three volcanic zones in the Kamchatka arc. Geochimica et Cosmochimica Acta 65, 4523–4537.
Jordan, B.T., Grunder, A.L., Duncan, R.A., Deino, A., 2004. Geochronology of age-progressive volcanism of the Oregon High Lava Plains: Implications for the plume interpretation of Yellowstone. Journal of Geophysical Research 109, B10202. doi:10.1029/2003JB002776.
Klochko, K., Kaufman, A.J., Yao, W., Byrne, R.H., Tossell, J.A., 2006. Experimental measurement of boron isotope fractionation in seawater. Earth and Planetary Science Letters 248, 276–285.
Leeman, W.P., 1988. Boron contents in selected international geochemical reference samples. Geostandards Newsletter 12, 61–62.
Leeman, W.P., 1999. Boron geochemical constraints on subduction contributions: Relations to slab thermal structure and other subduction parameters. EOS Transactions of the American Geophysical Union 80, F1182.
Leeman, W.P., Sisson, V.B., 1996. Geochemistry of boron and its implications for crustal and mantle processes. In: Grew, E.S., Anovitz, L.M. (Eds.), Boron Mineralogy and Geochemistry. Mineralogical Society of America Reviews in Mineralogy, vol. 33, pp. 645–708.
Leeman, W.P., Vitaliano, C.J., Prinz, M., 1976. Evolved lavas from the Snake River Plain: Craters of the Moon National Monument, Idaho. Contributions to Mineralolgy and Petrology 56, 35–60.
Leeman, W.P., Menzies, M.A., Matty, D.J., Embree, G.F., 1985. Strontium, neodymium and lead isotopic compositions of deep crustal xenoliths from the Snake River Plain: evidence for Archean basement. Earth and Planetary Science Letters 75, 354–368.
Leeman, W.P., Oldow, J.S., Hart, W.K., 1992. Lithosphere-scale thrusting in the western U.S. Cordillera as constrained by Sr and Nd isotopic transitions in Neogene volcanic rocks. Geology 20, 63–66.
Leeman, W.P., Tonarini, S., Chan, L.H., Borg, L.E., 2004. Boron and lithium isotopic variations in a hot subduction zone: the southern Washington Cascades. Chemical Geology 212, 101–124.
Leeman, W.P., Annen, C., Dufek, J., 2008. Snake River Plain–Yellowstone silicic volcanism: implications for magma genesis and magma fluxes. Geological Society of London, Special Publication 304, 235–259.
Leeman, W.P., Schutt, D.L., Hughes, S.S., 2009. Thermal structure beneath the Snake River Plain: Implications for the Yellowstone hot spot. Journal of Volcanology and Geothermal Research 188, 57–67.
leRoux, P.J., Shirey, S.B., Benton, L., Hauri, E.H., Mock, T.D., 2004. In situ, multiple-multiplier, laser ablation ICP-MS measurement of boron isotopic composition (d11B) at the nanogram level. Chemical Geology 203, 123–138.
Lowenstern, J.B., Hurwitz, S., 2008. Monitoring a supervolcano in repose: Heat and volatile flux at the Yellowstone caldera. Elements 4, 35–40.
MacLeod, N.S., Walker, G.W., McKee, E.H., 1976. Geothermal significance of eastward increase in age of upper Cenozoic rhyolite domes in southeastern Oregon. Second United Nations Symposium on the Development and Use of Geothermal Resources, Proceedings 1, pp. 465–474.
Marschall, H.R., Altherr, R., Rüpke, L., 2007. Squeezing out the slab — modelling the release of Li, Be and B during progressive high-pressure metamorphism. Chemical Geology 239, 323–335.
Marschall, H.R., Altherr, R., Kalt, A., Ludwig, T., 2008. Detrital, metamorphic and metasomatic tourmaline in high-pressure metasediments from Syros (Greece): intra-grain boron isotope patterns determined by secondary-ion mass spectrometry. Contributions to Mineralogy and Petrology 155, 703–717.
McCurry, M., Hayden, K.P., Morse, L.H., Mertzman, S., 2008. Genesis of post-hotspot, A-type rhyolite of the Eastern Snake River Plain volcanic field by extreme fractional crystallization of olivine tholeiite. Bulletin of Volcanology. doi:10.1007/s00445-007-0143-4.
Nabelek, P., Denison, J., Glascock, M., 1990. Behavior of boron during contact metamorphism of calc–silicate rocks at Notch Peak, Utah. American Mineralogist 75, 874–880.
Nash, B.P., Perkins, M.E., Christensen, J.N., Lee, D.C., Halliday, A.N., 2006. The Yellowstone hotspot in space and time: Nd and Hf isotopes in silicic magmas. Earth and Planetary Science Letters 247, 143–156.
Oldow, J.S., Bally, A.W., Avé Lallemant, H.G., Leeman, W.P., 1989. Phanerozoic evolution of the North American Cordillera. In: Bally, A.W., Palmer, A.R. (Eds.), The geology of North America: An overview. Geology of North America, vol. A. Geological Society of America, Boulder, Colorado, pp. 139–232.
Palmer, M.R., Sturchio, N.C., 1990. The boron isotope systematics of the Yellowstone National Park (Wyoming) hydrothermal system: A reconnaissance. Geochimica et Cosmochimica Acta 54, 2811–2815.
Palmer, M.R., Swihart, G.H., 1996. Boron isotope geochemistry: an overview. Mineralogical Society of America. Reviews in Mineralogy and Geochemistry, vol. 33, pp. 709–744.
Pennisi, M., Leeman, W.P., Tonarini, S., Pennisi, A., Nabelek, P.I., 2000. Boron, Sr, O, and H isotope geochemistry of groundwaters from Mt. Etna (Sicily) — hydrologic implications. Geochimica et Cosmochimica Acta 64, 961–974.
Pierce, K.L., Morgan, L.A., 1992. The track of the Yellowstone hot spot—volcanism, faulting and uplift. In: Link, P., Kuntz, M., Platt, L. (Eds.), Regional geology of eastern Idaho and western Wyoming. Geological Society of America Memoir, vol. 179, pp. 1–53.
Rudnick, R.L., Gao, S., 2004. Composition of the Continental Crust. In: Holland, H.D., Turekian, K.K. (Eds.), Treatise on Geochemistry, 3. Elsevier, Amsterdam, pp. 1–64.
Ryan, J.G., Leeman, W.P., Morris, J.D., Langmuir, C.H., 1996. The boron systematics of intraplate lavas: Implications for crust and mantle evolution. Geochimica et Cosmochimica Acta 60, 415–422.
Savov, I.P., Tonarini, S., Ryan, J., Mottl, M., 2004. Boron isotope geochemistry of serpentinites and porefluids from Leg 195, Site 1200, S. Chamorro Seamount, Mariana forearc region. International Geological Congress (IGC), Florence, Italy.
Savov, I.P., Ryan, J.G., D'Antonio, M., Fryer, P., 2007a. Shallow slab fluid release across and along the Mariana arc-basin system: Insights from geochemistry of serpentinized peridotites from the Mariana Forearc. Journal of Geophysical Research 112, B09205. doi:10.1029/2006JB004749.
Savov, I.P., Cai, M.Y., Shirey, S.B., Ryan, J.G., Hauri, E.H., Goldstein, S.L., Navarro-Ochoa, C., 2007b. Is new Plinian Eruption Imminent at Colima Volcano in Mexico? Insights From Mineral Chemistry, Melt Inclusion Volatiles and Bulk Rock B–Li–Sr–Nd–Hf–Pb Isotopic Systematics. Fall Meet. Suppl., Abstract V31H-06. *Eos* Trans. AGU, vol. 88 (52).
Schmitt, A.K., Simon, J.I., 2004. Boron isotopic variations in hydrous rhyolitic melts: A case study from Long Valley, California. Contributions to Mineralogy and Petrology 146, 590–605.
Schmitt, A.K., Kaseman, S., Meixner, A., Rhede, D., 2002. Boron in central Andean ignimbrites: Implications for crustal boron cycles in an active continental margin. Chemical Geology 183, 333–347.
Shaw, D.M., Truscott, M.G., Gray, E.A., Middleton, T.A., 1988. Boron and lithium in high-grade rocks and minerals from the Wawa-Kapuskasing region, Ontario. Canadian Journal of Earth Sciences 25, 1485–1502.
Spivack, A.J., Palmer, M.R., Edmond, J.M., 1987. The sedimentary cycle of the boron isotopes. Geochimica et Cosmochimica Acta 51, 1939–1949.
Streck, M.J., Grunder, A.L., 2007. Phenocryst-poor rhyolites of bimodal, tholeiitic provinces: The Rattlesnake Tuff and implications for mush extraction models. Bulletin of Volcanology 70. doi:10.1007/s00445-007-0144-3.
Tamura, Y., Tatsumi, Y., 2002. Remelting of an andesitic crust as a possible origin for rhyolitic magma in oceanic arcs: an example from the Izu-Bonin arc. Journal of Petrology 43, 1029–1047.
Taylor, H., Sheppard, S., 1986. Igneous rocks; I, Processes of isotopic fractionation and isotope systematics. Reviews in Mineralogy and Geochemistry 16, 227–271.
Tiepolo, M., Bouman, C., Vannucci, R., Schwieters, J., 2006. Laser ablation multicollector ICP-MS determination of δ^{11}B in geological samples. Applied Geochemistry 21, 788–801.
Tonarini, S., Leeman, W.P., Pennisi, M., Ferrara, G., 2001. Boron isotopic variations in lavas flows of the Aeolian volcanic arc, Italy. Journal of Volcanology and Geothermal Research 110, 155–170.
Tonarini, S., Leeman, W.P., Leat, P.E., 2004. Boron isotope systematics in South Sandwich island arc. Geochimica et Cosmochimica Acta 68, A599 [Abst. 15th Goldschmidt Conference, Copenhagen, Denmark].
Willbold, M., Stracke, A., 2007. Trace element composition of mantle end-members: Implications for recycling of oceanic and upper and lower continental crust. Geochemistry, Geophysics, Geosystems 7, Q04004. doi:10.1029/2005GC001005.
You, C.F., Chan, L.H., Spivack, A.J., Gieskes, J.M., 1995. Lithium, boron, and their isotopes in sediments and pore waters of Ocean Drilling Program Site 808, Nankai Trough: implications for fluid expulsion in accretionary prisms. Geology 23, 37–40.